

CAUSTIC-LIKE STRUCTURES IN UHECR FLUX AFTER PROPAGATION IN TURBULENT INTERGALACTIC MAGNETIC FIELDS

K. Dolgikh^{a,b}, *A. Korochkin*^{c,b}, *G. Rubtsov*^{a,b}, *D. Semikoz*^d, *I. Tkachev*^{a,b*}

^a *Institute for Nuclear Research of the Russian Academy of Sciences
117312, Moscow, Russia*

^b *Physics Department and Laboratory of Cosmology and Elementary Particle Physics,
Novosibirsk State University
630090, Novosibirsk, Russia*

^c *Université Libre de Bruxelles
1050, Brussels, Belgium*

^d *APC, Université Paris Cité, CNRS/IN2P3, CEA/IRFU,
Observatoire de Paris
119 75205, Paris, France*

Received October 20, 2022,
revised version December 1, 2022
Accepted for publication December 2, 2022

DOI: 10.31857/S0044451023060044
EDN: DEDUQZ

UHECR propagation in a turbulent intergalactic magnetic field in the diffusion regime is well understood for propagation distances much larger than the field coherence scale, see e.g. Refs. [1–4]. The diffusion theory doesn't work and unexpected effects may appear for propagation over smaller distances, from a few and up to 10–20 coherence scales [5–7]. We study the propagation of UHECRs in this regime, which may be relevant for intermediate mass UHECR nuclei and nG scale intergalactic magnetic fields with 1 Mpc coherence scale. We found that the trajectories form a non-trivial caustic-like pattern with strong deviation from isotropy. Thus, measurements of the flux from a source at a given distance will depend on the position of the observer.

In general, deflections of cosmic rays in a turbulent field with coherence length λ_C as a function of distance has three regimes. At $D < \lambda_C$, the deflection occurs across the main direction of the magnetic field in the given region. As a result, the deflection grows almost

linearly $\theta = (D/D_0)^\alpha$ with $\alpha = 0.9$ in our case. For $D > 5\lambda_C$ deflections occur in diffuse regime and a typical power law corresponds to $\alpha = 0.5$. Therefore, for $D \gg \lambda_C$ and small deflection angles

$$\theta \sim 4^\circ Z \frac{B}{\text{nG}} \frac{10 \text{ EeV}}{E} \sqrt{\frac{D}{\text{Mpc}}} \sqrt{\frac{\lambda_C}{\text{Mpc}}},$$

where Z is the atomic number of the primary particle. Finally, in the intermediate regime $\lambda_C < D < 5\lambda_C$, and on average, the exponent α is interpolated between the above values.

However, averaging can erase important properties of UHECR propagation at a given distance from the source, and two-dimensional slices of the density distribution of cosmic rays propagating from a source have never been studied. In this work, medium-scale anisotropies are revealed in a certain range of parameters in the two-dimensional distribution of cosmic rays on spheres around the source.

The physical reason for the appearance of anisotropies during propagation in a turbulent field can be understood analytically. In [6] it is shown that in the case of initially parallel proton beam, inhomogeneities in the particle distribution are caused

* E-mail: tkacheff.igor2015@yandex.ru

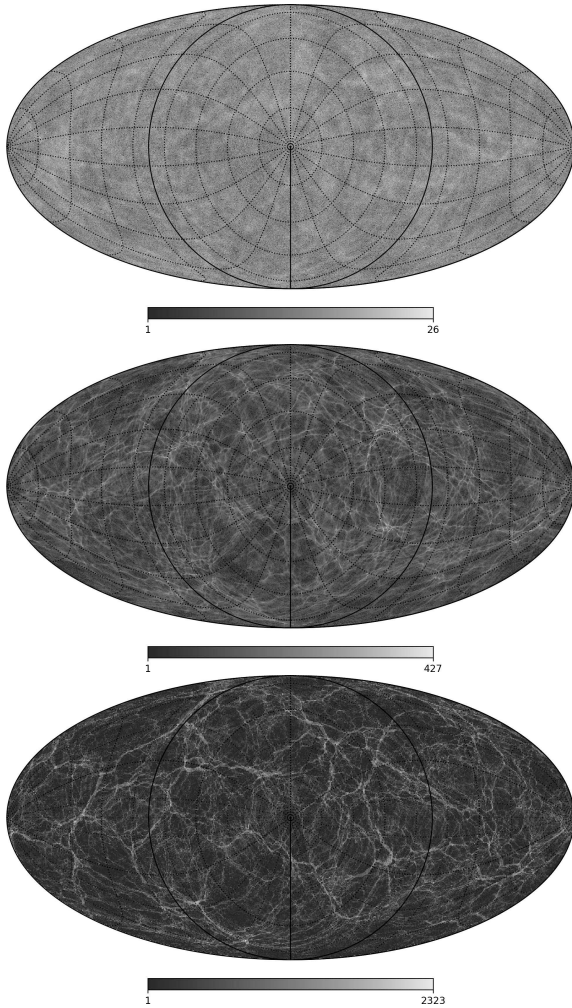


Fig. 1. UHECR distribution on a sphere with a radius of 10 Mpc. From top to bottom, the magnetic field was turned off after 1,3,10 correlation lengths, respectively.

by fluctuations of the magnetic field rotor along the trajectories of neighbouring particles. Namely, the cross-sectional area $A(D)$ of the particle beam trajectories turns out to be linearly dependent on the magnetic field rotor [6]. In the case of a diverging beam, results of Ref. [6] should be modified due to different beam geometry, which determines different initial conditions. We have used corresponding initial conditions and have derived the equation for the diverging beam:

$$A(D) = A_0 \left(1 - \frac{Ze}{E} \int_0^D s \left(1 - \frac{s}{D} \right) (\text{rot} \vec{B} \cdot d\vec{s}) \right). \quad (1)$$

It should be noted that the equations are valid only for small amplification $(A(D) - A_0)/A_0 \ll 1$ and small deflections of particles. Rewriting Eq. (1) in terms of

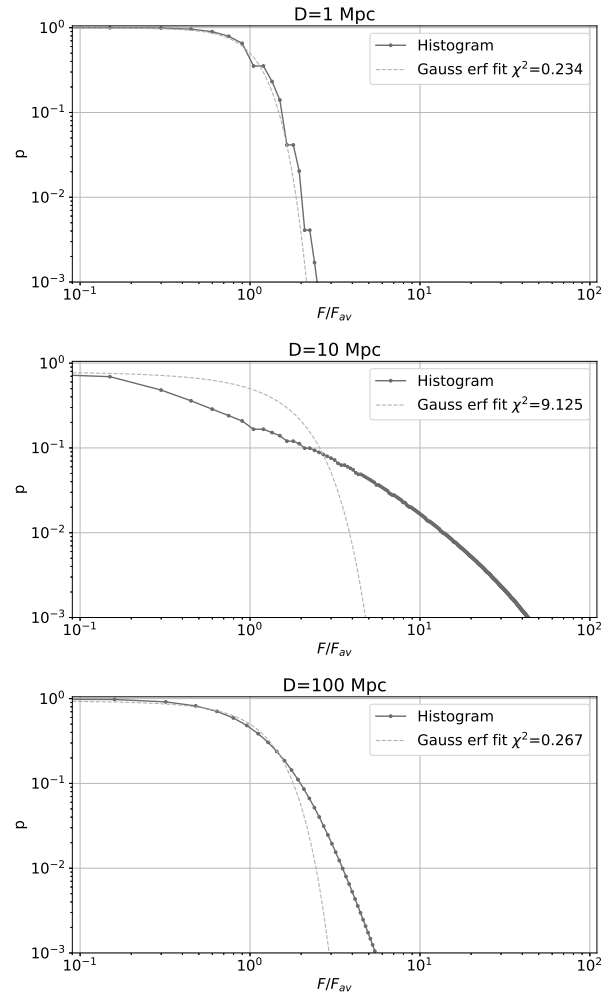


Fig. 2. The cumulative probability of detecting an above-average flux on a sphere with a radius of 1, 10 and 100 Mpc from the source. At a distance close to the Larmor radius, the distribution is strongly non-Gaussian.

the number of particles N , we arrive to a relation that can be verified directly in numerical simulations:

$$\frac{\Delta N}{N} = \frac{1}{R_L} \left[\frac{\int_0^D s(D-s)(\text{rot} \vec{B} \cdot d\vec{s})}{DB} \right], \quad (2)$$

where R_L is a Larmor radius.

We use publicly available codes `CRbeam` [9] and `CRPropa` [10, 11] for cosmic ray propagation. All interactions and cosmological expansion of the Universe are turned off. The particles were emitted isotropically and propagated until they reached a sphere of a given radius D . The resulting output is processed with the package `healpy` [12, 13].

In Fig. 1, lower panel, we show a sky map with UHECR density at a fixed radius of the sphere around the source. This figure shows an example of a UHECR with $E = 10$ EeV propagating in a turbulent magnetic field with strength $B = 1$ nG and coherence scale $\lambda_C = 1$ Mpc. With such a field and energy of cosmic rays, we expect that the maximum anisotropy in the UHECR distribution will be reached at 10 correlation lengths, i.e. at a distance of $D = 10$ Mpc. The bar under the figure shows the color correspondence to the density of cosmic rays in the structures. Three types of structures can be identified: knots with the highest density, filaments and voids with the lowest density. Note that the typical size of a magnetic field domain with $\lambda_C = 1$ Mpc has an angular scale of 6-10 degrees on this map and corresponds to small features. However, the most prominent and highly visible are the medium-scale structures, with a typical scale of about 60 degrees. To understand the angular scale of these structures, we have shown in Fig. 1 the UHECR density at $D = 10$ Mpc, but when the magnetic field is set to zero outside the 1 and 3 Mpc spheres, see top and middle panels respectively. It can be seen that most of the global structure observed at a distance of 10 Mpc is formed during the passage of the first 3 correlation lengths from the source, its physical size corresponded to the correlation length at that time. Later on the structure mainly sharpens.

By randomly changing the location of the observer, we calculate the cumulative probability of detecting a flux above a given value which is shown in the Fig. 2. The x-axis is normalized to the mean density on the sphere. We plot the cumulative probability at a distance of 1, 10, and 100 Mpc from the source, from the top panel to the bottom, respectively. Both at small and large distances, the probability distribution is similar to Gaussian. However, in the middle panel it is very far from Gaussian. The probability of getting a flux below average is 80%. At this distance from the source, the initial flux is likely to decrease, e.g. by a factor of 10 with a probability of about 20%. The probability of an order of magnitude gain is only 2% .

Finally, we have verified that the appearance of caustic-like structures does not depend on specific parameters of the magnetic field spectrum. In particular, our results are robust to changes in the ratio of maximum and minimum turbulence scales.

Conclusions. In this work, we have studied the propagation of UHECRs in a turbulent intergalactic magnetic field in the small-angle scattering regime. We

found that even if UHECRs are emitted isotropically from their source, they are distributed anisotropically at a distance of the order of the Larmor radius, and again isotropically at a distance 10 times greater. The enhanced regions merge into a filamentary, caustic-like structure on the sphere. The angular arrangement of these regions is dictated by the structure of the magnetic field at several coherence lengths from the source.

The relative size of the enhanced regions depends on the coherence length of the magnetic field. This anisotropic distribution can affect the UHECR spectrum at distances from the source comparable to the Larmor radius. In addition, this can also lead to the formation of hot spots in the observer's distribution of cosmic rays over the sky, and can also affect the ratio between the number of observed hot spots and the density of UHECR sources.

Funding. Work of K.D., A.K., G.R. and I.T. was supported by the Russian Science Foundation grant 20-42-09010. The work of D.S. has been supported by the French National Research Agency (ANR) grant ANR-19-CE31-0020.

The full text of this paper is published in the English version of JETP.

REFERENCES

1. F. Casse, M. Lemoine, and G. Pelletier, *Phys. Rev. D* **65**, 023002 (2016).
2. G. Giacinti, M. Kachelriess, and D. V. Semikoz, *Phys. Rev. Lett.* **108**, 261101 (2012).
3. G. Giacinti, M. Kachelriess, and D. V. Semikoz, *JCAP* **07**, 051 (2018).
4. D. Harari, S. Mollerach, and E. Roulet, *Phys. Rev. D* **93**, 063002 (2016).
5. D. Harari, S. Mollerach, and E. Roulet, *JHEP* **10**, 047 (2000).
6. D. Harari, S. Mollerach, and E. Roulet, and F. Sanchez, *JHEP* **03**, 045 (2002).
7. K. Dolag, M. Kachelriess, and D. V. Semikoz, *JCAP* **01**, 033 (2009).
8. D. Harari, S. Mollerach, and E. Roulet, *JHEP* **08**, 022 (1999).

9. V. Berezhinsky and O. Kalashev, *Phys. Rev. D* **94**, 023007 (2016).
10. R. Alves Batista, A. Dundovic, M. Erdmann, Karl-Heinz Kampert, D. Kuempel, G. Müller, G. Sigl, A. van Vliet, D. Walz, and T. Winchen, *JCAP* **05**, 038 (2016).
11. R. Alves Batista et al., *JCAP* **09**, 035 (2022).
12. A. Zonca, L. Singer, D. Lenz, M. Reinecke, C. Rosset, E. Hivon, and K. Gorski, *Journal of Open Source Software* **4**, 1298 (2019).
13. K. M. Górski, E. Hivon, A. J. Banday, B. D. Wandelt, F. K. Hansen, M. Reinecke, and M. Bartelmann, *Astrophys. J.* **622**, 759 (2005).
14. J. Giacalone and J. R. Jokipii, *Astrophys. J.* **520**, 204 (1999).